International Conference on Space Optics—ICSO 2022

Dubrovnik, Croatia

3–7 October 2022

Edited by Kyriaki Minoglou, Nikos Karafolas, and Bruno Cugny,

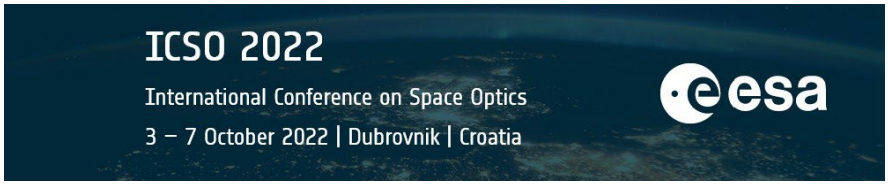

Space-grade Gallium Arsenide IQ and Modulator Arrays for VHTS Photonic SatCom Systems

International Conference on Space Optics — ICSO 2022, edited by Kyriaki Minoglou, Nikos Karafolas, Bruno Cugny, Proc. of SPIE Vol. 12777, 127777C · © 2023 ESA and CNES · 0277-786X · doi: 10.1117/12.2691388

Space-grade Gallium Arsenide IQ and Modulator Arrays for VHTS Photonic SatCom Systems

Robert Walker, Nigel Cameron, Yi Zhou, Stephen Clements
aXenic Limited, Thomas Wright Way, Sedgefield, Durham TS21 3FD, UK

ABSTRACT

We discuss the design and implementation of compact IQ modulators and modulator arrays to be monolithically integrated in the GaAs/AlGaAs material system. Considerations are presented for the design of GaAs traveling-wave electro-optic modulator arrays for space data-link applications. Central to the modulator design is a low loss folded optical configuration giving direct, straight-line RF access at one end of the device, with all fiber-optical ports at the opposite end. This configuration is a critical enabler for the close-packed monolithic modulator arrays needed for multi-channel applications. It also leads to much more compact packaging, improved fiber handling and contributes to high modulation bandwidths with low ripple by eliminating directional change in the RF feed arrangements. Typically, the folded devices are half the length of conventional format modulators and a modest array of devices (e.g. x4) can be accommodated in a package of similar dimensions to a single modulator. Design considerations for arrays of independently addressed MZ modulators (each with its own input fiber) are discussed. Both single MZ and monolithic dual-parallel (IQ) modulators have been assessed up to 70GHz, with bandwidths of 40-50GHz achieved with a low-frequency Vπ below 3V. A novel integrated RF termination, of especial benefit to a compact array configuration, is demonstrated with return loss better than 12dB to 70GHz.

Keywords: fiber optics, electro-optic modulators, modulator arrays, DQPSK, 50GHz, GaAs, AlGaAs, III-V semiconductor.

1. INTRODUCTION

With the rise of VHTS, the satellite market must move towards new techniques and technologies – specifically opto-electronic (O/E) – to realize the vastly increased data capacities envisaged. The EU H2020 *SIPhoDiAS* program targets this requirement, aiming to advance O/E componentry in performance, size and power while enhancing reliability towards TRL7.

There are clear advantages to be gained from the enormous data capacity of multiplexed optical links, and with RF frequencies progressing towards Q/V bands. Electro-optic modulators are viewed as a *Critical Space Technology* for microwave photonic payloads by the European Space Agency [1], with increasing interest in frequencies of 50GHz and higher. Modulator arrays based on the capabilities reported here will feed into the *SIPhoDiAS* project.

The environmental credentials of gallium arsenide in the GaAs/AlGaAs III-V semiconductor material system are well known; the large semiconductor bandgap yields environmental stability and a useful degree of radiation tolerance [2]. This makes it a natural choice for space-borne systems, with many desirable properties for RF devices which must survive and operate in harsh environments.

Traveling-wave electro-optic modulators in GaAs have similar properties of linearity to the better-known lithium niobate devices but can access higher bandwidths and lower drive-voltages within a significantly more compact footprint as well as offering enhanced stability. There is of interest not only in discrete modulators, but also in arrays and composite devices for modulation formats such as single-sideband (SSB) and quadrature phase-shift key (QPSK). Both SSB and QPSK coding can be produced using a dual parallel *IQ* modulator, which is essentially a x2 modulator array (or x4 for the dual-polarization variant) with added optical split and recombine elements.

2. GAAS ELECTRO-OPTIC MODULATORS

The Mach-Zehnder modulator (Figure 1) consists of a parallel pair of electro-optic phase modulator waveguides, fed by an optical splitter, differentially driven, and finally recombined to the device output. The phase modulators, shown in cross-section in the inset of Figure 1, use the vertical E-field set-up between the top Schottky electrode and a doped backplane which is grown into the epitaxial layers beneath the waveguides.

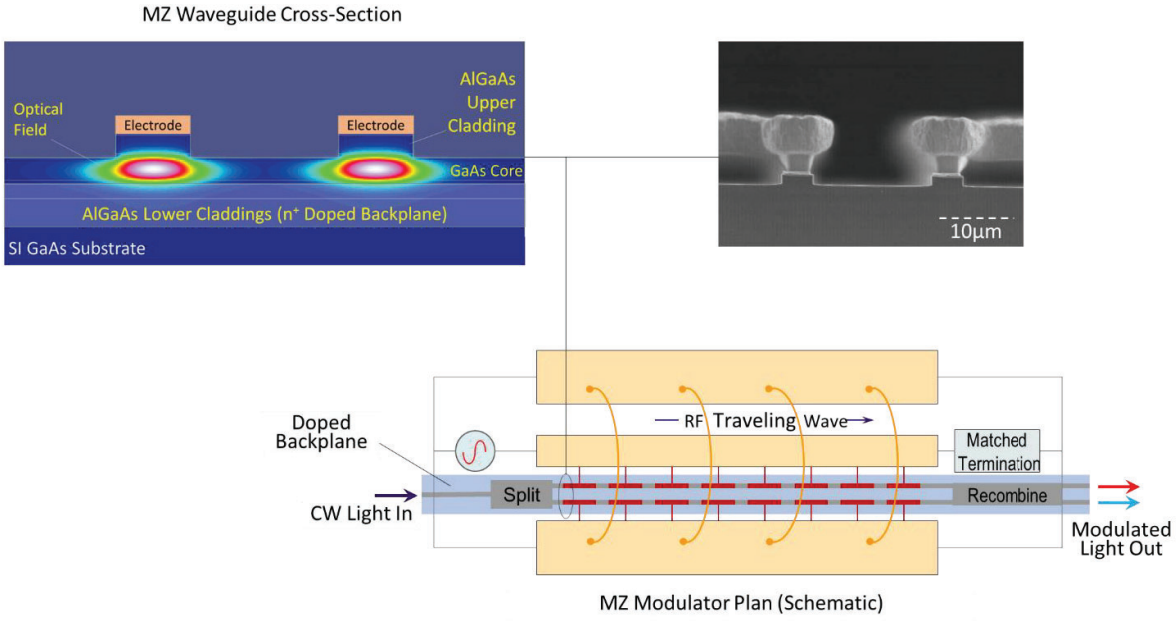

Figure 1 Schematic GaAs/AlGaAs loaded-line traveling wave modulator based on ground-strapped CPW transmission-line.
Top left: waveguide cross-section with optical simulations (scalar field)
Top right: SEM micrograph showing rib waveguides with electrodes and plated air-bridges

The E-field, utilizing the linear electro-optic effect, is efficiently overlapped with the guided optical profile which is itself optimally confined by the GaAs/AlGaAs refractive-index contrast vertically and by the etched rib horizontally. Since the phase-modulators are inherently connected back-to-back by the doped backplane, they naturally operate in a series push-pull mode [3],[4]. The applied RF potential divides equally between the waveguides, producing balanced, anti-phase contributions to the modulation, and with an effective capacitance which is half that of each individual branch.

Optical recombination produces a raised-cosine output-intensity function with no net phase modulation (i.e. zero chirp) and characterized by the half-wave (ON-OFF) voltage $V\pi$. Since the device is interferometric, it operates by routing and apportioning the light between two complementary outputs (dependent on the relative phase at the inputs to the recombiner). One of the outputs is commonly used to monitor and control the bias condition.

2.1 RF Design and Velocity Matching

Since the linear electro-optic effect in most materials is weak, the modulators need to be quite long (e.g., 20-30 mm active length) to achieve a suitably low drive voltage. This length requirement is what drives the need for a velocity-matched traveling-wave configuration; simple 'lumped' electrodes of such a length cannot achieve modulation bandwidths above a few hundred MHz. Analysis shows that this limitation is mainly due to interfering antiphase modulation due to reflected RF from the open ends of the electrodes [5]. Accordingly, a main feature of a traveling-wave design is that RF is launched at one end of the electrode (rather than the center). The electrode pair is treated as a transmission-line and the reverse RF wave is suppressed by means of a matched termination, which is usually around 50Ω. The termination is usually an external lumped component, but if this function *can* be integrated into the modulator itself, there are advantages in doing so – especially for a modulator array. This is discussed further in 2.3 below.

In addition, the ideal is to match the velocity of the RF wave to the velocity of the optical modulation group which it is generating. If these can be kept in step, the modulation will accumulate monotonically along the entire length of the electrode. In semiconductor materials the bulk permittivity is similarly valued at optical and RF frequencies; the optical group-index is about 3.55 at 1550nm in GaAs while the RF dielectric constant is about 13, giving an RF (refractive) index of 3.605. This *should* make velocity-matching very easy; however, in a coplanar transmission-line, loading from the air superstrate averages down the effective dielectric constant to about 7 (RF Index 2.65 at low frequency) whereas the optical profile, being fully buried, retains something like the bulk value.

The *capacitively loaded line* configuration used by our modulators is a slow-wave structure in which the modulation electrodes are segmented as a set of short quasi-lumped elements isolated by passive spaces (Figure 1). These sample the line-voltage to accumulate phase-modulation while also adding net capacitance to the transmission-line which slows the progression of the RF wave.

The *slow-wave factor* is related to the ratio of electrode and coplanar cross-sectional capacitance values [5], thus:

$$Slow\_wave\ Factor = \sqrt{1 + {}^{C_L}/_{C_c}} \tag{1}$$

where C_L is the loading capacitance due to the electrodes, and C_c is the unloaded coplanar capacitance (both per unit length)

The required slow-wave factor is around 1.34 (= 3.55/2.65) in GaAs. Since this same factor also applies to characteristic impedance, an unloaded coplanar impedance of 67Ω would also be loaded down to the standard 50Ω of the system.

Because of RF dispersion – a progressive increase in RF index with frequency – the slow-wave factor above (with fixed C_c) is only strictly applicable at low frequencies. CPW (coplanar waveguide) has lower RF dispersion and loss than other coplanar transmission-line types and so is preferred despite the added complication of twin ground-planes, which must be cross-connected periodically by bond-wires (or substrate vias) to suppress higher-order RF mode generation. Dispersion is influenced by many factors but is also increased by periodic structures such as the segmented electrodes and CPW ground-plane bonding shown in Figure 1.

When designing the modulator, dispersion is accommodated by targeting velocity-matching at the highest frequency of interest. Typically, the RF velocity is set-up to be 'fast' at low frequency where velocity mismatch is less important, allowing RF dispersion to establish velocity-match at the higher frequency.

RF loss and dispersion ultimately place limits on the high frequency performance which generally favor shorter devices with tighter field confinement and higher electro-optic slope-efficiency. A tendency for this to increase the *optical* insertion loss is ameliorated by the fact that the optical paths within the device are also shorter. System loss is generally agnostic to such distinctions, being a composite of optical loss and dynamic Vπ, so a holistic design process seeks to optimize the overall system performance at the highest frequency of interest.

2.2 Folded Modulator Topology

It is clear from the schematic of Figure 1, that the input requirements for the RF and the light are potentially in conflict. It is not practical to launch both the light and the RF at (or near) the same point on the periphery of the GaAs chip. Conventionally, the RF ports are located on the sides of the device with the RF routed through 90° coplanar bends while the optical line is kept essentially straight. We refer to this conventional configuration as *In-Line* from the optical arrangement.

For frequencies much above 30GHz, this is not good enough – and this is one reason for our emphasis on optical path-folding, which allows the RF input-run to be as short and straight as possible while the *optical* paths are folded using compact 90° bends as illustrated in Figure 2 below. This concept requires low loss optical waveguide corner-bends as discussed in 3.2. In an array-compatible topology, a common optical I/O facet must be at the opposite end to the RF inputs; the lateral sides of all but the outermost units are inaccessible to RF or optical I/O.

In addition to performance advantages, the folded device can be made much more compact. The active electro-optic interaction length is enabled to fill most of the available length while DC control electrodes can utilize at-least some of the input-run (see Figure 5 later).

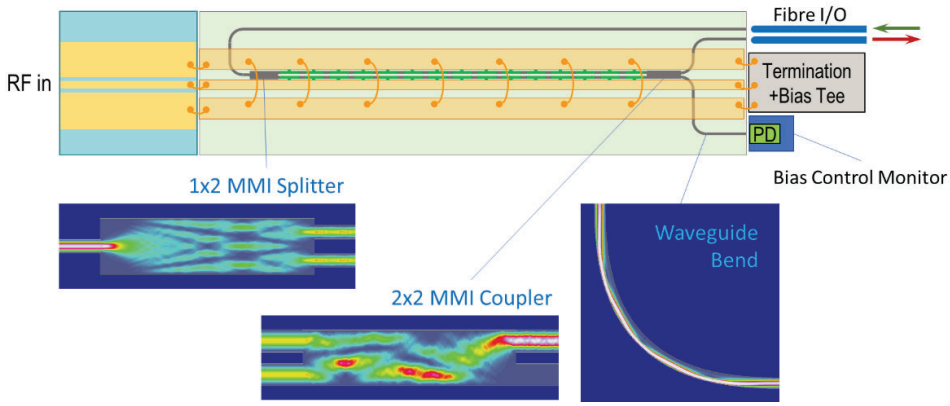

Figure 2 Folder MZ modulator configuration, illustrating MMI and corner-bend simulations.

Finally, there are configurational advantages for the system in terms of fiber handling when all fibers are at the same end of the device. Even internally, within the modulator package there are gains in compactness due to the concentration of space-hungry fiber interfaces at one end. The folded-optics topology is particularly suitable for phased-array applications with fiber-optic antenna-head remoting.

Both single MZM and dual 'IQ' devices of this type have been demonstrated. For example, Figure 3 compares measured frequency responses for fully packaged single modulators using both *In-Line* and *Folded* approaches. The devices use a similar waveguide and electrode design. These active RF lengths differ which complicates the comparison; nevertheless, the degree of HF response extension in the folded 50GHz device is striking.

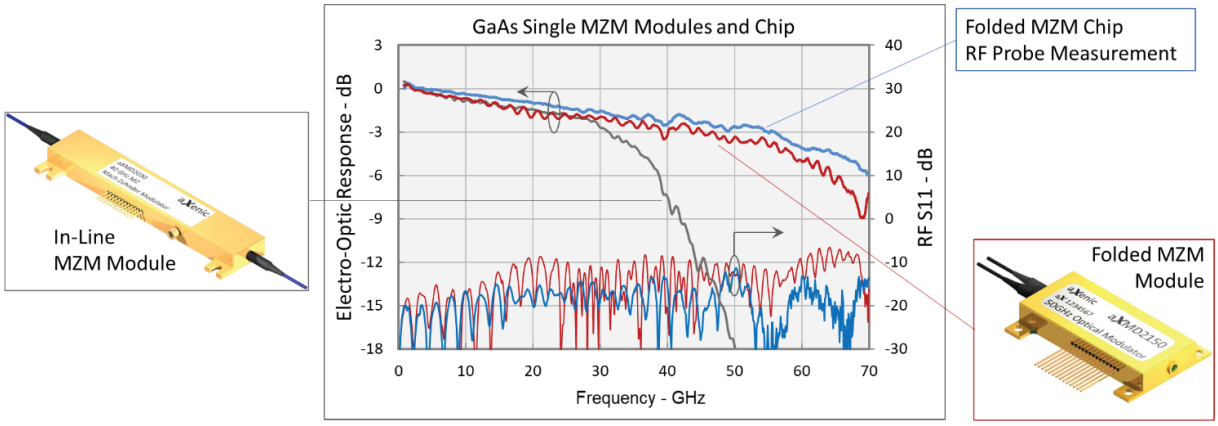

Figure 3 Folded and In-Line MZM performance to 70GHz.
Red: Folded Module: 45mm package length (18mm active); Vπ=4.6 at 1550nm
Blue: Unpackaged folded MZ chip (as Red), RF probed measurement.
Grey: In-Line GaAs module: 30mm active, 78mm package length; Vπ=3 at 1550nm

The folded design (package length: 45mm) achieves 45 GHz bandwidth with Vπ below 5V. The compared In-Line module, with package length 78mm is an older design with Vπ of 3V and 30GHz bandwidth.

The folded module is also compared with the initial probed chip-on-carrier response. Performance is generally reduced by RF interfacing aspects, an issue pertinent to RF interfacing aspects of array design, as discussed in section 4.1

2.3 Integrated RF Termination

In the modulator array context, an external RF termination competes for space with the optical fiber coupling arrangements and must be connected (with wire-bonds) to the end of the RF transmission-line. This inevitably produces an RF discontinuity with reflections which rise with frequency; wire-bonds over an airgap are generally inductive.

There are obvious benefits to be accrued from on-chip integrated RF termination:

- Better return loss figure because there are no inductive bond-wires.
- Saving on cost, parts inventory and assembly time/effort.
- Placed immediately at the end of the active section, the on-chip region near the end-facet is freed for optical detail.
- The off-chip area at the facet is left clear for the critical fibre interfacing arrangements. This is especially important for an *NxN* array where multiple fibres must be accommodated.

An integrated termination has been successfully realized as shown in Figure 4. A baseline criterion was that this must be fabricated entirely within the native gallium arsenide foundry process with no new process steps or materials required. Therefore, the termination comes at zero additional cost. The lack of an ohmic contact process to the doped backplane led to the concept outlined here, with some compromise on performance considered acceptable to comply with this criterion. Nevertheless, the design appears to be thoroughly successful, rivalling off-chip ceramic termination components in performance.

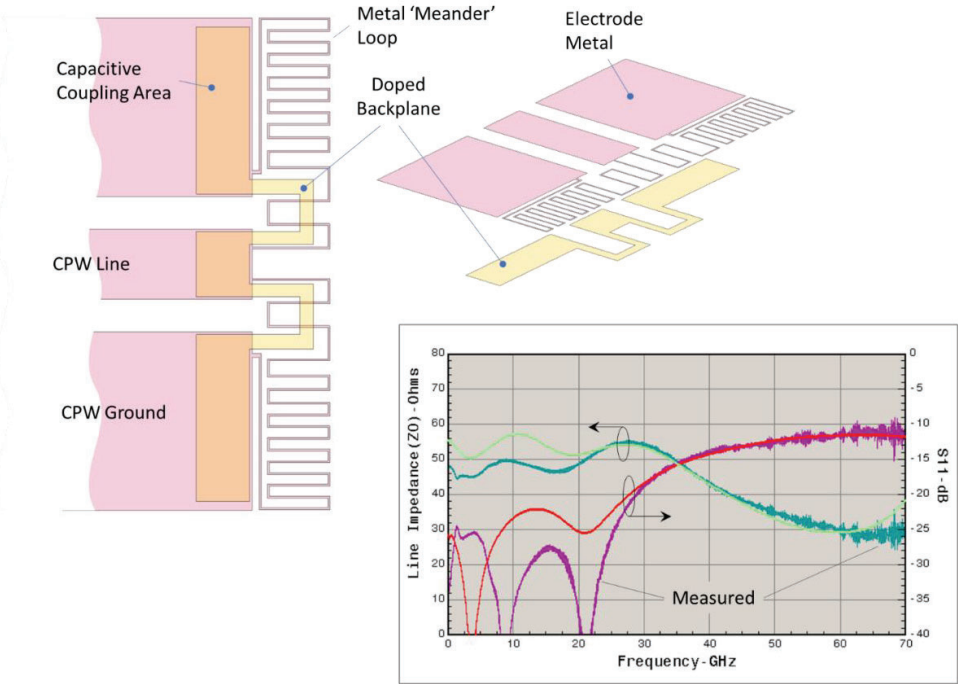

Figure 4 Integrated RF termination (plan and exploded 3D) with simulated and measured result

The termination comprises both metallic and semiconductive contributions arranged in parallel. The former is created as a serpentine 'meander' of standard electrode metallization; since this is inductive and is directly connected to the CPW line it primarily handles low-frequency RF components. The second contribution comprises a pair of 'U' bridges patterned in the existing doped backplane layers of the epitaxy; this is capacitively coupled to the CPW line and mainly handles high frequency components. Distributed cross-couplings – some unavoidable, some intentional – between these two systems help smooth the crossover band.

The termination was designed for 50Ω. The accuracy of the realization of this impedance is conditioned by the consistency of the materials used. The electrode metal used for the low frequency 'meander' is a standard foundry Ti:Pt:Au formulation

which is well controlled (and routinely assessed for sheet resistance) and is found to provide a reliable resistivity. The high frequency 'U' bridge resistance is conditional upon the sheet resistance of the epitaxial layers. This is a specified parameter of the epitaxial growth but being dependent on growth conditions seems more prone to variability and dependent on the growth technique. In practice, the higher frequencies are already attenuated by the active section of the modulator, so this is generally less critical.

The measured result, also shown in Figure 4 was obtained from a directly probed test drop-in, but similar units integrated with modulators appear to behave similarly; full device tests are pending. As can be seen there is good agreement between the simulation and the measured result.

2.4 Layout Schemes for Modulator Arrays

The folded-optical methods aid and promote the extension of GaAs modulator technology to more advanced configurations, such as IQ modulators, used for QPSK and single sideband formats, as well as monolithic arrays of modulators. Here, we consider the most general and versatile *NxN* arrays where each unit of the array has its own independent input fiber rather than a possible *IxN* alternative with one input fiber and an integrated 1xN splitter.

The *NxN* array encourages a modular approach, with identical MZM units and independent fiber I/O blocks. The main part of Figure 5 illustrates a 2x2 dual modulator unit, arranged as a mirror-pair, which supports the use of a single x4 fiber I/O block serving both MZM elements. Alternatively, the unit MZM can be step repeated, rather than mirrored, using individual x2 fiber I/O blocks to produce a truly modular array concept, as also shown in Figure 5 (right). Modular layouts are versatile and clearly there is no impediment to repeating this to create x4, x6, x8 ... modulator arrays.

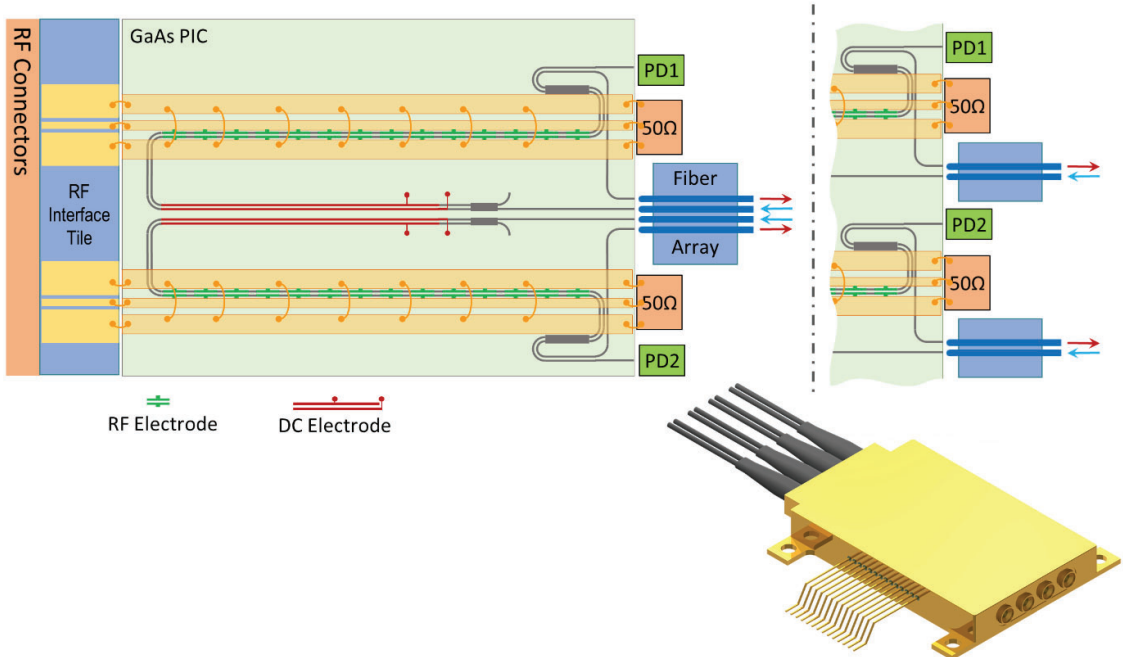

Figure 5 Folded-path modulator arrays (Schematic – not to scale).
Left: 2x2 array unit with x4 fiber I/O block;
Right: Alternative I/O detail for using x2 fiber-blocks.

2.5 Fiber Interfaces

Modulators being designed for arrays within the *SIPHoDiAS* program are expected to perform similarly to the existing single and IQ devices. A significant undertaking is the extension of (or development of new) techniques for low-loss fiber interfacing. This is based on polarization-maintaining (PM) fiber and silicon V-groove mounting blocks. Currently individual fiber blocks are routinely aligned with low loss and high stability. Extending this to 2 or 4 fibres in a single

silicon block will be challenging due to the simultaneous multiple alignments that will be required. Fibres must be aligned to micron tolerances longitudinally, but for managing arrays of polarization maintaining fiber they must also be aligned to within a degree axially.

As already indicated, modular arrays with optical ports local to the MZM unit favor fiber interfaces based on *N-fold* 2-fiber blocks (In+Out). Aligning a 2-fiber block will be somewhat more difficult than aligning a single fiber, but routes also exist to extend this approach to a larger number of fibers in a single block. Choice of the best combination of size of the arrays in terms of fibers and the accuracy of alignment for each fiber will depend on the criticality of factors such as cost, through monolithic integration of larger chips and those of performance, most notably excess alignment loss.

3. GAAS OPTICAL WAVEGUIDE TECHNOLOGY

Our GaAs modulator technology is built upon an industry-standard pHEMT, rules-based foundry process. The fabrication sequence starts with six-inch semi-insulating GaAs wafers upon which the epitaxial layers are grown by one of the standard technologies (MBE or MOCVD). Contactless projection steppers are used for optical waveguide and electrode photolithography. A dry Reactive Ion Etch (RIE) process ensures that deep-etched waveguide ridge walls finish within 2° of vertical. This is the only step that deviates from the standard pHEMT sequence and is based on a frontside-to-backside via process, modified to ensure the edge acuity required for low scattering loss and the verticality.

Thin metal electrodes are deposited by e-beam evaporation and standard lift-off techniques prior to waveguide definition. This is a standard Ti:Pt:Au stack that ensures good adhesion and conductivity and provides a rectifying Schottky contact due to the undoped upper layers of the epitaxy. Low loss RF transmission-lines and air-bridge contacts to the electrodes are established after the RIE etching by gold electro-plating to a thickness of at least 5µm.

3.1 Waveguides

Both shallow ‘rib’ and deep ‘ridge’ types of waveguide are used within the device for different purposes. Rib waveguides are used where single-mode behavior is required, for fiber-matched I/O, and for the electro-optic sections where the shallower etch is required by foundry design-rules for air-bridge contacts. The deep-etched ridge type is etched fully through the GaAs core-layer and features a very high ‘air-wall’ lateral index-contrast. The nearly vertical walls minimize polarization conversion by the bends which are so important a feature of our designs.

Deep and shallow (or ‘strong’ and ‘weak’) waveguide sections are coupled by low-loss taper transitions which have been found to contribute no more than 0.05dB loss [3]. Because of the smooth ridge walls produced by the foundry RIE process, the scattering loss of the two waveguide types is found to be similar, typically at 0.25dB/cm.

3.2 Matched Corner Bends

The folded-optics device concept requires bends that contribute almost no optical loss or net mode-coupling. The waveguides used for the bend-sections are of the deep-etched ridge type, with behavior dominated by mode-coupling and mode-interference mechanisms rather than by radiative loss. Our designs are based on the concept of the *matched bend*, in which the total path-length is matched to a dominant intermodal beat-length, with gradation of curvature [3] to modulate the mode excitation.

While it is possible to devise single-function U or S bends it is more usual – and generally better – to simply concatenate standard optimized bends – mainly 90° ‘corners’ (Figure 2 includes a simulation), but 45° bends also find application. Optimization of a bend-profile is not based on simple best loss performance but on worst-case net mode-coupling over a range of anticipated process and wavelength variation.

Losses of multi-bend concatenations and other waveguide test structures are measured by a fabry-perot resonance technique [6] using test-pieces with uncoated end-facets. The excess loss per bend is typically found to be between 0.012dB and 0.02dB, averaging about 0.015dB and with very low sensitivity to wavelength [7].

3.3 Couplers, Splitters and Recombiners

Most guided-wave optical circuits will require splitters and recombiners to perform basic interferometry. Historically, Y-branches and waveguide directional-couplers were the go-to structures for these functions (and this is still the case for lithium niobate modulators based on diffused channel waveguides). However, these structures require a mono-mode,

weakly-confining waveguide to function properly, which in-turn leads to excessive process sensitivity and generally low compatibility with a compact folded geometry which is based on strong ridge waveguides.

The preferred split/combine solution is based on the well-known Multimode Interference (MMI) element [3],[8]. These are lengths of wide, deep-ridge waveguide with suitably placed waveguide ports. Figure 2 illustrates MMI splitter and coupler simulations.

The MMI concept uses the fact that the guided (plus radiation) modes of a waveguide form a complete orthogonal set, so any launch profile can be analyzed as a superposition of these modes. A sequential relationship between the phase velocities of the modes ensures that the initial condition recurs cyclically at multiples of a fundamental beat-length along the MMI waveguide. Consequently, a lens-like re-imaging of the launch profile results. The double image that appears at half this re-imaging length provides 2x2 split and recombination functions. Other multiple image points on a centrally excited MMI can provide a high precision, low loss 1xN split, potentially useful for a 1xN modulator array.

The deep-ridge waveguide properties are generally stable, giving the MMI a good process and environmental tolerance. Thus, MMIs are eminently manufacturable, though sensitive to factors that might affect the intermodal beat-lengths (primarily wavelength and width). The sensitivity manifests as a loss increase away from the design centre; unlike the directional coupler (for example), the split ratio is generally maintained. The tight (±0.1μm) dimensional tolerance provided by the GaAs foundry process may result in a 'red' or 'blue' shift of the loss-minimum wavelength by up to 10nm. A typical well-centered MMI splitter operates over a 1520nm – 1580nm operational band with only ~0.15dB excess loss at either end of the range while the ±0.1μm process width range has a similar impact mid-band at 1550nm.

3.4 Optical Power Taps and Mode Filters

The basic 1x1 full re-imaging of an input waveguide to an identical output waveguide does not appear at first sight to be very interesting. However small MMIs of this type make frequent appearances in our designs for ancillary functions such as odd-order mode filtering, low-level optical power-taps and low-loss crossovers.

Optical power-taps are an ancillary requirement for bias control which is still required despite the relative stability of the GaAs material system. Control based on a low frequency pilot-tone may be intrusive in some systems in which case a ratioing system may be preferred, requiring low-level signals tapped from the input and output. This can be done in fibre but is more cost and space/weight effective done on-chip.

There is a dearth of attractive alternative options for optical power-taps. Those previously considered include:

a) Directional couplers, comprising close-spaced waveguides running parallel, or possibly just converging and immediately diverging again (either way, the necessary curving convergence and divergence contributes significantly to the coupling and must be allowed for in the design). The problem for III-V rib/ridge waveguides is that stable, deep-etched waveguides show almost no mutual coupling unless impracticably close-set while for shallow-etched rib waveguides, the coupling is very sensitive to the etch, and to wavelength.
b) Asymmetric Y-junctions
c) Special MMI configurations. These can provide unequal split-ratios [9], but not the low -10 to -20 dB tap levels we want. 'Barrel' and 'Butterfly' perturbations of 2x2 MMIs [9] are able to modify the usual 50:50 split-ratio – but, again, not provide the low tap levels without disturbance and loss to the main through-route.

Our novel design for low-level power-taps is based on the small 1x1 MMI which is frequently used as a mode-filter for odd-order modes. This MMI is a centrally excited and when designed to re-image the dominant waveguide mode to the similar output waveguide (with negligible loss) has the property of imaging all odd-order modes onto the 'shoulder' regions either side of the output. Thus odd-order modes – in particular the troublesome first-order mode – can be rejected.

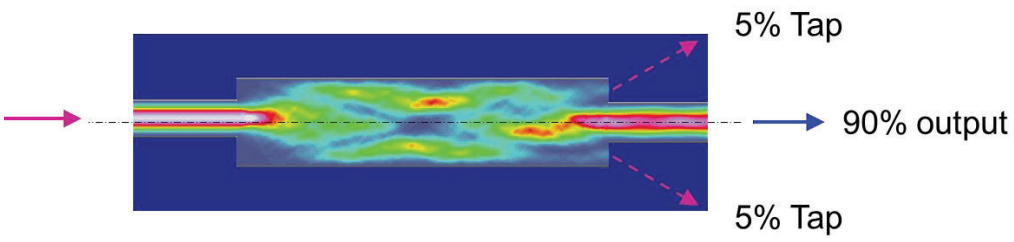

Figure 6 Simulation of modified mode-filter functioning as a 10% (-10dB) power-tap. Output shoulders can be angle-facetted to divert and combine the two tap signals

The power-tap design adds to this mode-filter thus:

a) By providing facetted shoulders to reflect the rejected light sideways to be collected by suitably placed waveguides.
b) By perturbing the input waveguide to intentionally create a controlled odd-mode component.

Modelling shows these power-taps to be stable over wavelength and essentially adiabatic, losing from the main path little more than the tap signal. Some of the latest modulator designs incorporate prototype power-taps of this type; they function as expected and appear not to add any significant excess loss.

4. IQ MODULATORS AND ARRAYS

IQ Modulators (IQMs) are a specialized form of two-fold array, with additional MMI couplers allowing both MZM units to be fed from a single input and coherently recombined onto a single output. Several evolutions of these have been realized in our GaAs/AlGaAs technology, with increasing refinement in bend, MMI and RF design. Earlier designs have been supplied into collaborative programs for system demonstrations, for example the European Seventh Framework program *Galactico*, where one was used to demonstrate 150 Gbit/s using 64 level QAM (Quadrature Amplitude Modulation) [10].

The latest of these designs [7] is essentially an IQ version of the folded MZ modulator shown in Figure 5. The RF and waveguide configuration is similar to that shown, but with the extra optical couplers, as noted above.

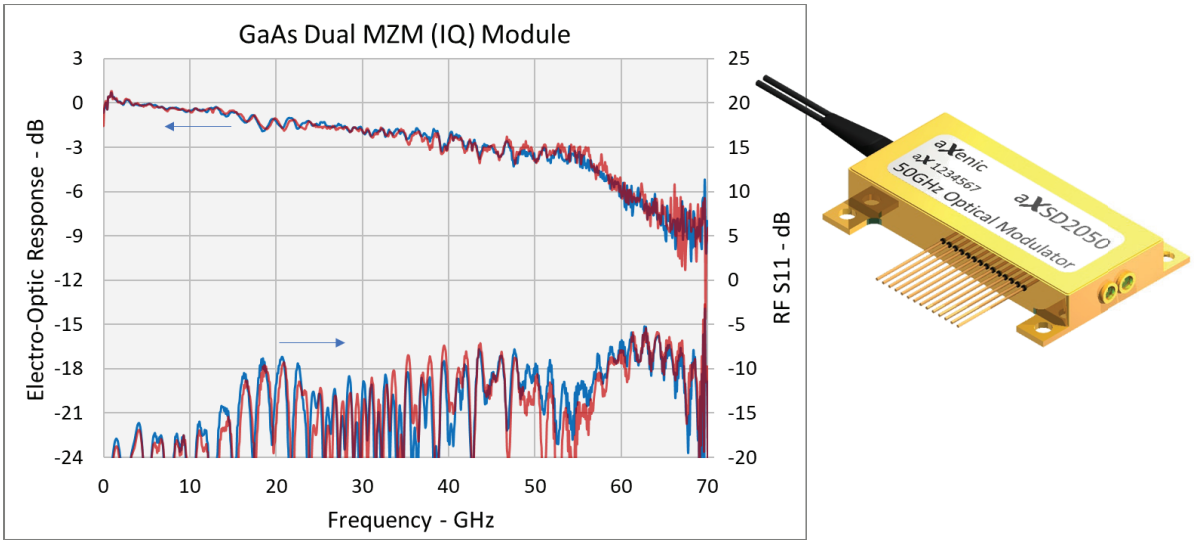

Figure 7 Measured electro-optic RF characteristics for folded-path GaAs IQ modulator module based on the 18mm configuration of Figure 3. Vπ=4.6 at 1550nm.

Measured responses for 'I' and 'Q' channels on a recent IQ device (fully packaged) are shown in Figure 7, demonstrating excellent channel balance with near identical RF modulation characteristics, which should be indicative of potential *NxN* modulator array performance. A similar module (supplied commercially) has recently been used to demonstrate 220 Gbaud signal generation [11].

IQ Modulators with Reduced Drive Voltage

A more recent iteration of this IQ modulator design uses a longer RF/optical interaction zone with reoptimized epitaxial layers aiming to achieve both lower Vπ and improved optical loss. Measured RF characteristics are shown below in Figure 8. The trade-off of RF bandwidth for lower Vπ is due both to the longer active zone and a reduced intrinsic (undoped) thickness (Figure 1). The design nevertheless produces a slightly larger optical spot which interfaces more efficiently to fibre.

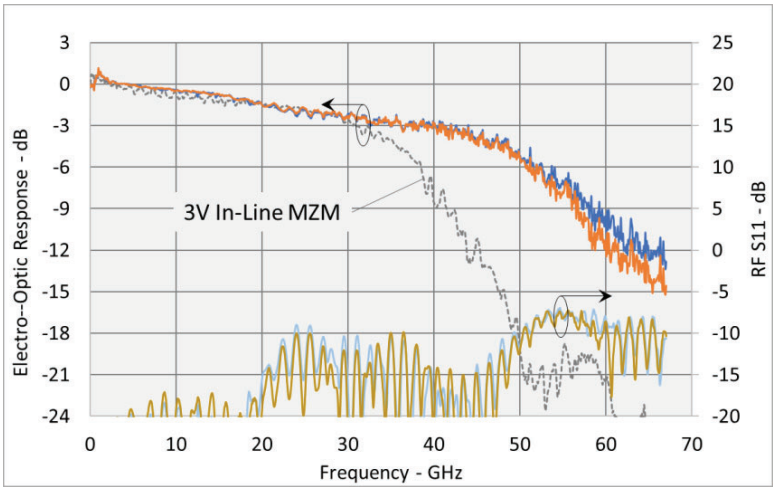

Figure 8 Measured electro-optic RF characteristics for an improved folded-path GaAs IQ module. Similar Vπ (2.85) to the early in-line module (reproduced from Figure 3 for comparison).

The DC Vπ for these devices has been measured at 2.85V which is close to that of the *In-Line* device featured in Figure 3 but significantly lower than the 4.6V of the shorter folded devices of Figure 7. Notably, the -3dB corner frequency is not much reduced – it falls to ~40GHz from ~45GHz; moreover, at 50GHz the dynamic Vπ remains significantly lower in the new device, at ~5V compared to ~7V.

The new design also incorporates some further RF refinements to improve S11. The channel balance up to 55GHz remains excellent while the RF return loss is better, and ripple is lower.

With the Vπ value now similar to that of the *In-Line* MZM featured in Figure 3 a fair comparison is now possible of the two devices. The impact of the intervening improvements is clear, with the straightened RF input, shorter RF interaction and a smaller electrode pitch mainly responsible for the extended RF response, while the improved epitaxial design permits a shorter interaction while still achieving a similar Vπ.

4.1 Channel Balance in Modulator Arrays

The degree of channel balance seen in Figure 7 and Figure 8 for an IQ modulator is relatively straightforward to achieve when there are only two channels, as mirror symmetry generally ensures this high degree of balance. There are, nevertheless, some non-idealities: some of the noise and ripple detail is measurement related - for example, due to imperfect de-embedding of the high-speed photodetector, cables, and RF adapters. Some response structure is added by the packaging, as is clear from Figure 3; typically, measurement of the unpackaged chip using a GSG RF probe system shows lower S_{11} and smoother EO response with higher bandwidth than does the final packaged module. Understanding of these issues is important to achieving well balanced multi-channel RF responses in a xN array where N is greater than 2.

Earlier work [2] on four-channel array-like devices (dual-polarization IQ modulators – DPIQMs) identified a clear 'inner' *versus* 'outer' dichotomy whereby the two outer and the two inner channels were well balanced, as expected from

symmetry, but the inner and outer were different. These DPIQM modulators were pitched on a repeat spacing which was significantly narrower than that of the RF connectors. This required an interface tile designed to achieve a 'fan-in', with tighter bending of the CPW outer channels and with path-balancing convolutions of the inner channels. The response imbalance above 30GHz was traced to these details.

Learning from this, *NxN* array designs should aim for perfect channel balance by pitching the MZM units on the same spacing as the RF connectors. The minimum spacing for SMP-M connectors is 3.6mm – a current OIF standard. For more economical use of the GaAs material and improved high-frequency specification, the smaller SMP-S connector can be adopted. Alternatively, the RF interface tiles can be arranged in mirror pairs with equal minimal bending of each CPW.

A further balance issue in the earlier DPIQM design was found to be due to the RF terminations being sited at the sides of the chip, requiring longer on-chip coplanar runs from the inner channels to the edge. Here, we have proposed that the RF terminations should at least be sited on the end-facet along with the optical interfaces as shown in Figure 2 and Figure 5. Better still, the termination can be integrated onto the chip as proposed in 2.3 (Figure 4). This keeps the end-facet clear for the critical optical interfacing arrangements.

5. CONCLUSIONS

Folded-optics, traveling-wave, GaAs electro-optic modulators have achieved 45GHz bandwidths (>50GHz unpackaged) with Vπ of 4.6V, while latest designs achieve 40GHz (packaged) with a Vπ of 2.85V. Both single and dual-parallel (IQ) configurations designed for 1550nm have been demonstrated. The latest design uses a new efficient epitaxial layer design to improve fibre interfacing and reduce Vπ with only a minor bandwidth impact. The folded optical configuration allows straight in-line RF access to the active section, contributing to high modulation bandwidths with low ripple by eliminating directional change in the RF feed arrangements. This also facilitates compact packaging and improves overall access by segregating the optical interfaces to one end of the module with the RF interfaces at the other end. The folded arrangement also leads to much more compact packages since the modulator chip is typically much shorter; moreover, the space-hungry fiber-interfacing arrangements are concentrated at one end, while considerations of RF loss encourage minimalist RF interfacing at the other.

The IQ modulator reported here is a specialized example of a generic 1x2 modulator array. This is readily extended to *NxN* arrays using the folded-optical methods outlined. Current packages have sufficient space for these larger arrays without needing to add to the width of the package. Ultimately, with larger arrays, the number and spacing of the RF connectors, rather than the optical chip size would be the main driver towards wider packages.

A novel on-chip integrated RF termination has been demonstrated with return loss better than 12dB up to 70GHz. This was implemented to assist in configuring modulator arrays by eliminating the external termination component.

Optical power monitoring is required to enable bias control of each modulator of an array. Novel power-tap structures have been demonstrated which can integrate this function almost losslessly on-chip.

Funding

The reported work was performed within the frames of H2020-SPACE-SIPHODIAS project. This project has received funding from the European Union's Horizon 2020 research and innovation program under grant agreement No 870522

References

[1] Technologies for European Non-Dependence and Competitiveness, SPACE-10-TEC-2018 (Guidance Document for Horizon 2020 Work Programme 2018-2020): *http://ec.europa.eu/research/participants/data/ref/h2020/other/guides_for_applicants/h2020-supp-info-space-10-18-20_en.pdf*

[2] Walker, R. G., Cameron, N., Zhou, Y., & Clements, S. (2017, September). "Electro-optic modulators for space using gallium arsenide", International Conference on Space Optics – ICSO, International Society for Optics and Photonics, Vol.10562, 105621A (2016)

[3] Walker, R. G., Cameron, N. I., Zhou, Y., & Clements, S. J., "Optimized gallium arsenide modulators for advanced modulation formats", IEEE Journal of Selected Topics in Quantum Electronics, 19(6), 138-149 (2013)

[4] Walker, R. G., "Broadband (6 GHz) GaAs/AlGaAs electro-optic modulator with low drive power," Applied Physics Letters, 54(17), 1613-1615 (1989)

[5] R. G. Walker and J. Heaton, "Gallium arsenide modulator technology" in Broadband Optical Modulators – Science, Technology and Applications, Boca Raton, FL: CRC Press, 2012, Chapter 8, pp. 207-221

[6] Walker, R. G., "Simple and accurate loss measurement technique for semiconductor optical waveguides", Electronics Letters, 21(13), 581-583,714 (1985)

[7] Robert Walker, Nigel Cameron, Yi Zhou, Chris Main, Gary Hoy, Stephen Clements, "50GHz gallium arsenide electro-optic modulators for spaceborne telecommunications", Proc. SPIE. 11180, International Conference on Space Optics — ICSO 2018

[8] Soldano, L. B., and Pennings, E. C., "Optical multi-mode interference devices based on self-imaging: principles and applications", Journal of Lightwave Technology, 13(4), 615-627 (1995)

[9] Besse, P.A.; Gini, E.; Bachmann, M.; Melchior, H., "New 2×2 and 1×3 multimode interference couplers with free selection of power splitting ratios", Journal of Lightwave Technology, 14(10) , 2286-2293 (1996)

[10] Schindler, P.C.; Korn, D.; Stamatiadis, C.; O'Keefe, M.F.; Stampoulidis, L.; Schmogrow, R.; Zakynthinos, P.; Palmer, R.; Cameron, N.; Zhou, Y.; Walker, R.G.; Kehayas, E.; Ben-Ezra, S.; Tomkos, I.; Zimmermann, L.; Petermann, K.; Freude, W.; Koos, C.; Leuthold, J., "Monolithic GaAs Electro-Optic IQ Modulator Demonstrated at 150 Gbit/s With 64QAM", Lightwave Technology, Journal of , vol.32, no.4, pp.760,765, Feb.15, 2014

[11] Pittalà, F., Schaedler, M., Khanna,G., Calabrò, S., Kuschnerov, M.,Xie, C., Ye,Z., Wang, Q. and Zheng, B., "220 GBaud Signal Generation Enabled by a Two-channel 256 GSa/s Arbitrary Waveform Generator and Advanced DSP", (2020), ECOC2020, SC5 PD24 (90P8PL4V05)